This is a repository copy of *FDTD modeling of heatsink RF characteristics for EMC mitigation* .

White Rose Research Online URL for this paper:
http://eprints.whiterose.ac.uk/806/

FDTD Modeling of Heatsink RF Characteristics for EMC Mitigation

Nick J. Ryan, *Member, IEEE*, Barry Chambers, *Senior Member, IEEE*, and D. A. Stone

Abstract—Due to their size and complex geometry, large heatsinks such as those used in the power electronics industry may enhance the radiated emissions produced by the circuits employing them. Such enhancement of the radio frequency (rf) radiation could cause the equipment to malfunction or to contravene current EMC regulations. In this paper, the electromagnetic resonant effects of heatsinks are examined using the finite-difference time-domain (FDTD) method and recommendations are made concerning the optimum geometry of heatsinks and the placement of components so as to mitigate potential EMC effects.

Index Terms—FDTD, heatsinks, radio frequency.

Fig. 1. Radiated emissions from an inverter drive measured at 3 m.

I. INTRODUCTION

THE recent implementation of the EU directive on EMC along with other international standards has meant that manufacturers of electrical and electronic systems have had to take EMC into consideration at every stage of the design process. Many items of equipment have had to be redesigned and some items have been withdrawn from sale after failing to meet standards. Designing for EMC is not a straightforward matter since many factors have to be taken into consideration. As a product becomes more complex, the potential for unfavorable interaction between different components increases, as does the potential for the equipment to produce unwanted radio frequency (RF) emissions.

In modern power electronics, switching systems are becoming commonplace. These systems are prone to producing large amounts of electromagnetic interference (EMI) in the form of high-order harmonics of the switching frequency and broadband semiconductor reverse recovery noise. This EMI is illustrated in Fig. 1, which shows part of the spectrum of emissions from a currently available inverter drive complying to European EMC standards. Even though the switching frequency of the drive is of the order of tens of kilohertz, emissions up to 900 MHz can clearly be seen. In power electronic systems it is common practice to solve the problem of EMC by screening and filtering. Perfect screening, however, is seldom possible, since the screen must often be compromised to allow for the routing of supply and control cabling. Another area in which screening is often compromised is the heatsink. The electronics generating much of the noise are the power semiconductors, and these devices need to be kept within a
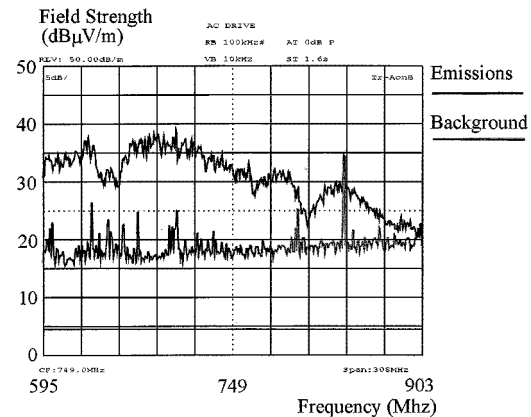
certain operating temperature range to ensure their continued operation; this is normally achieved by the use of heatsinks. For thermal reasons, the switching devices are either coupled directly to the metal heatsink or closely coupled via a thin insulating washer. Therefore, in most cases, any electrical noise produced by the device may be coupled directly to the heatsink. The use of screening attached to the heatsink may prevent some of the EM radiation, but this can be expensive and impede the airflow, and, thus, the performance of the heatsink. In some equipments, such as those employing the T03 package, the device is mounted on the external side of the heatsink. In more expensive applications, heatsinks are mounted internally and forced air cooling is used, and it is, therefore, inexpensive mass-produced items which are most problematic. Thus, devices generating high-frequency harmonics of switching currents are frequently mounted onto a large metallic object with potential multimode resonant characteristics.

Lee *et al.* [1] and Brench [2] have already shown that heatsinks can enhance the radiation produced by VLSI circuits, and using a finite-difference time-domain (FDTD) model, the authors have demonstrated multimode resonant behavior in power heatsinks [3], [4]. Power heatsinks differ from VLSI heatsinks in that the latter are made in only one or two standard geometries to fit directly over the VLSI device; thus, designers have little influence over the position of the source in relation to the heatsink. Conversely, power heatsinks come in many different sizes and geometries, and a designer may have to place tens of devices on any one heatsink, each one of which may act as a source of electromagnetic radiation. In this paper, we use the FDTD model to detail some of the mechanisms by which radiation enhancement occurs in power heatsinks and make recommendations to designers about the geometry

of the heatsink and component placement to avoid such enhancement. The FDTD model is introduced in Section II, and some if its features are discussed. Individual parameters are then investigated to determine electromagnetic resonance in power heatsinks. Section III summarizes the approach taken by the authors for this study. In Section IV, the effects of source position are examined, Section V discusses the geometry of the heatsink, while Section VI examines the effects of fins on the heatsink. Overall observations are made regarding the radiation characteristics of specific heatsinks in Section VII. Finally, the factors which should be borne in mind when using heatsinks are discussed in Section VIII and recommendations are made concerning the geometry of heatsinks and the orientation of fins and components.

II. FDTD METHOD

The FDTD method is based on the discretization of the electric and magnetic fields over rectangular grids, together with the finite-difference approximation of the spatial and temporal derivatives appearing in the differential form of Maxwell's equations. Originally proposed by Yee in 1966 [5], the FDTD method has gained great popularity in the past ten years as ever more powerful computers have become readily available, thus enabling more realistic electromagnetic problems to be investigated.

The standard FDTD technique divides the computational space up into cubic cells with the electric (E) and magnetic (H) fields discretised in the manner of these cells. The two-field types are offset by half a cell in such a way that every component of the electric field is surrounded by orthogonal magnetic components, and every magnetic field component is surrounded by orthogonal electric ones. The electric fields are assigned to integer time steps (n), whilst the magnetic fields are assigned to integer values plus one half of the time step $(n + 1/2)$; thus, the two-field types are intermeshed in time as well as in space. Next, the spatial and temporal derivatives of Maxwell's curl equations are approximated using second-order centered finite differences. The result is six expressions representing the electrical and magnetic field components in three dimensions. As an example, the expression for the E_z-field component is shown in

$$
\begin{aligned}
E_z|_{i,j,k}^{n+1} = C_a(m) \cdot E_z|_{i,j,k}^n + C_b(m) \\
\cdot \begin{pmatrix} H_y|_{i+1/2,j,k}^{n+1/2} - H_y|_{i-1/2,j,k}^{n+1/2} \\ +H_x|_{i,j-1/2,k}^{n+1/2} - H_x|_{i,j+1/2,k}^{n+1/2} \end{pmatrix}.
\end{aligned} \quad (1)
$$

The notation in (1) is that used by Taflove, [6] who gives a very thorough treatment of the development of the mesh. Heatsinks are often regular structures that are Cartesian by nature and can be easily and accurately represented in a three-dimensional Cartesian mesh. One of the strengths of the FDTD method is the fact that the model runs in the time domain, which allows for simultaneous multifrequency analysis. All of the models discussed here, used a pulse excitation to examine the behavior across a broad range of frequencies. The pulse excitation was derived by applying an exponential rise and decay to a sinusoidal signal with a zero-crossover point at the peak of the ex-
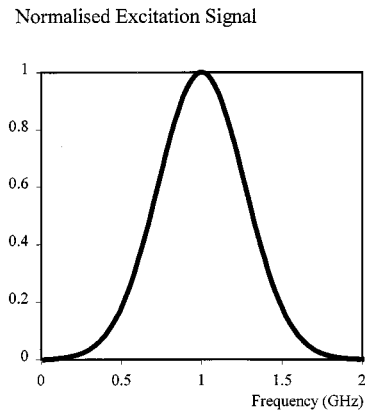

Normalised Excitation Signal

Fig. 2. Frequency response of the pulsed excitation used in the model.

ponential. The time domain waveform of the excitation pulse is given by

$$
E_{\text{source}} = \exp\left(\frac{-(n\Delta t - 3\tau)^2}{\tau^2}\right) \cdot \sin(\omega_{\text{cent}}(n\Delta t - 3\tau)). \quad (2)
$$

The frequency response can be centered on any frequency by changing the value of ω_{cent} and made broader by reducing or narrower by increasing the value of τ, as illustrated in Fig. 2 with $\tau = 100$, centered about 1 GHz. In all of the studies presented here, the source used is an ideal Herzian dipole implemented along a single FDTD grid edge. In a previous study comparing modeled results to measured data [4], a more complex source was used, whereby a small plate, representing the metal tag of a typical TO22 device, was coded into the mesh. A co-axial line, the center conductor connecting to the plate and the outer conductor connecting to the heatsink, was then used to excite this plate. This was found to give very similar results to the Herzian dipole excitation used in this paper. The scheme used for termination of the spatial boundaries of the mesh is the second-order boundary condition proposed by Mur [7]. In the problems discussed in this paper, the signal levels are large compared with reflections from the boundary, so, although this boundary condition is not the best available, it is well proven and without high computational overheads. A near-to-far-field conversion routine after that proposed by Luebbers *et al.* [8] has been used to gain far-field data.

III. APPROACH

The many different types of heatsink available and methods of component mounting produce a very complex problem with many parameters. The methodology used in this paper is to simplify the problem by examining only one or two parameters at a time. The results from each case are examined to compile a set of rules which may then be applied to heatsinks in general. Initially, the problem was simplified by reducing the heatsink to a single dimension; effectively a single piece of wire. This is investigated to find the ideal position for the source. The problem was then extended into two dimensions to analyze the effects of length versus width of the plate. Finally, the third Cartesian dimension was included to allow fins, blocks, and other more complex geometries in the heatsink structure.
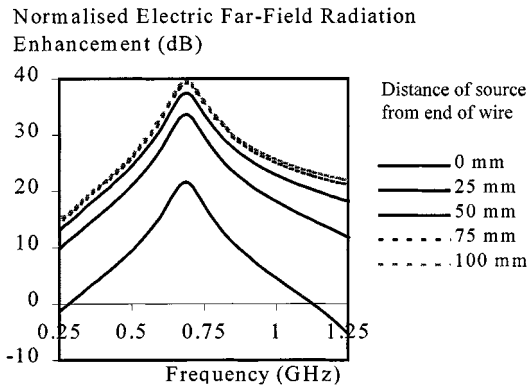
Fig. 3. Normalized radiation enhancement from a wire of 200 mm length with E-field excitation in the direction of the wire.

Fig. 4. Normalized radiation enhancement from a wire of 200 mm length with E-field excitation perpendicular to the direction of the wire.

Fig. 5. Radiation enhancement from a 200-mm long sheet of varying width.

IV. PLACEMENT AND ORIENTATION OF THE SOURCE

Reducing the problem to a single dimension simplifies the solid heatsink to a single thin wire representation, and this allows the effects of source position (distance from the end of the wire) and orientation (perpendicular or parallel to the wire) to be examined. It also allows comparison with known theoretical solutions, thus increasing the confidence in the software. A thin PEC wire was coded into the mesh and an excitation applied at different points. The far E-field radiation from the wire was calculated and normalized to that produced by an idealized dipole within an otherwise empty mesh. Initially, electric and magnetic dipoles either perpendicular or parallel to the thin wire were modeled. Note that the model displays rotational symmetry about an axis along the length of the wire. The results for the electric dipole are given in Figs. 3 and 4. In both cases, the frequency of the maximum radiation enhancement was slightly lower than the half wavelength frequency (0.75 GHz), corresponding to an infinitesimally thin dipole of the same length as the wire (200 mm). Hockanson *et al.* [9] have shown that a thin wire represented in an FDTD mesh by setting a single line of elements to zero yields effective wire radii of 20% of the cell dimension for cubic cells. The cell length used to model the wire was 5 mm, resulting in a wire with an effective diameter of 2 mm. Figs. 3 and 4 show the modeled resonant frequency of the wire to be 0.69 GHz which corresponds to a half wavelength of 217 mm. Burberry [10] has reported on the percentage increase in length due to fringing fields at resonance as a function of wavelength/diameter for the half-wave dipole; in this case, a change in length of approximately 8%. A reduction in the half wavelength of 8% results in a resonant length of 200 mm, which is the length of the modeled dipole.

Figs. 3 and 4 show how moving the source position affects the excitation of the dipole. The resonant frequency remains the same, but the level of excitation changes. In the case of the source acting in the direction of the wire (Fig. 3), enhancement was greatest with the source positioned at the center of the wire. In the case where the source was perpendicular to the wire (Fig. 4), enhancement was greatest with the source positioned at the end of the wire. The magnetic dipole excitation produced similar results to the electric dipole excitation of orthogonal orientation. The cas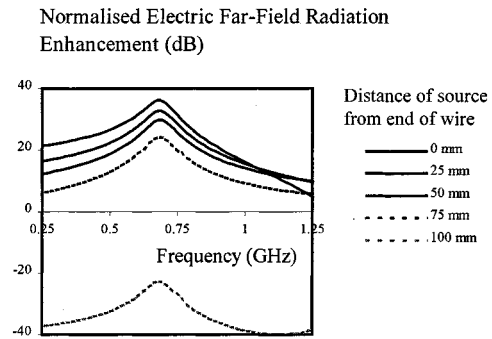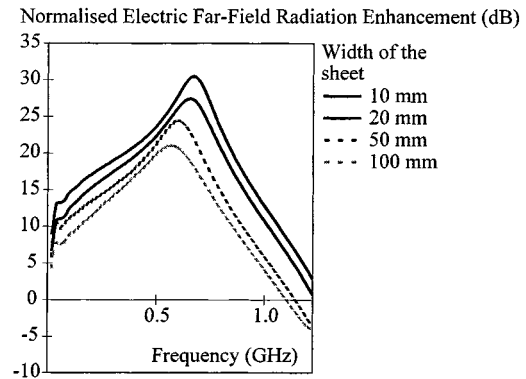es which led to maximum resonance were those which produced a differential field about the center of the wire. This behavior was also confirmed by examination of the near field.

The behavior of the half-wave dipole has been covered extensively in the literature, and the far-field may be calculated by assuming that the dipole is made up of elemental short dipoles and then integrating the response along the length of the antenna. This method makes the assumption that the current along the dipole is sinusoidal; this is a satisfactory approximation if the conductor diameter is small, say, $\lambda/200$ or less [11]. Applying an asymmetric excitation to the dipole, it is possible to calculate the response that this will have on the resonance of the dipole [10]. By comparison to such analytical results it is possible to validate the accuracy of the chosen method of numerical modeling.

V. HEATSINK GEOMETRY

It is very unlikely that a thin wire would be used as a heatsink, but extending the problem to two dimensions produces a flat plate, the simplest of practical heatsinks. This type of heatsink is often used as a common baseplate or chassis for the mounting of components and PCBs. In a practical circuit, there will be many sources of emissions, both electric and magnetic, acting on such a plate. One of the most common, and the easiest to identify, is that caused by capacitive coupling from components mounted onto the heatsink. When components are mounted onto the heatsink and insulated from it by a small plastic washer, the washer becomes a dielectric layer between two metal plates, the tag of the device, and the heatsink. This results in a high-intensity E field forming between the parallel plates, normal to the
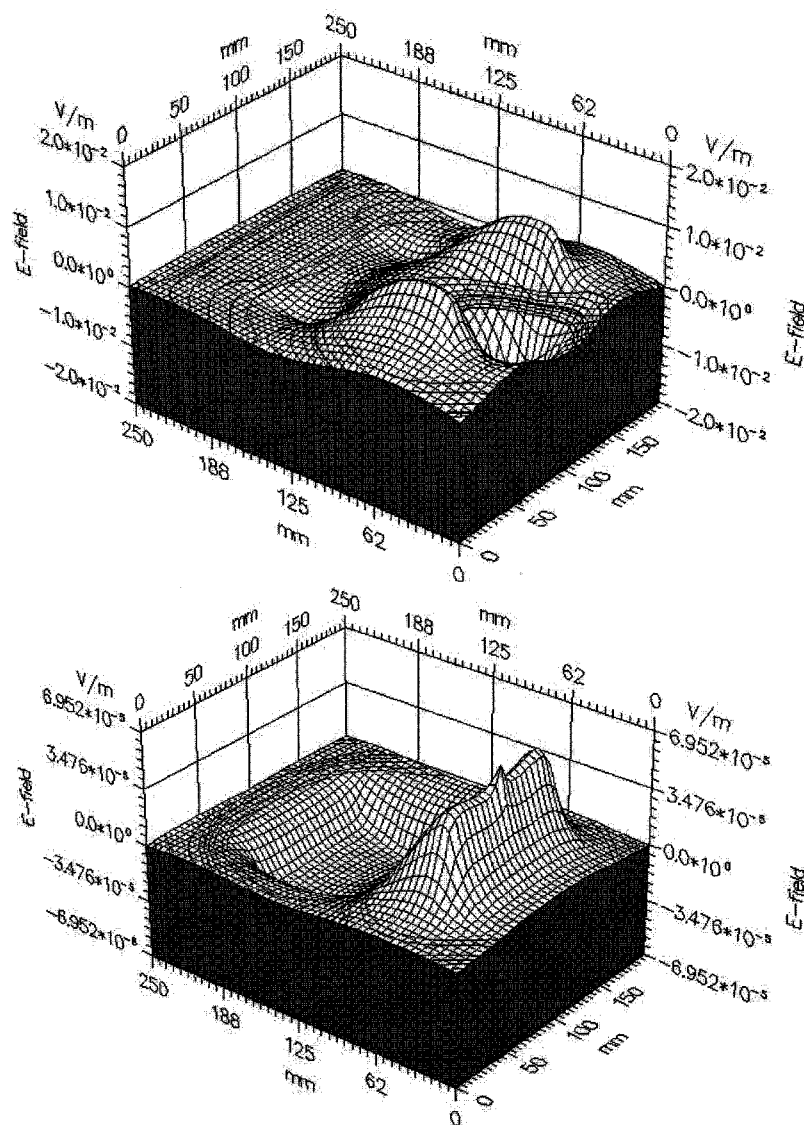
Fig. 6 (a) *E*-field diagram seen above sheet a sheet 150 by 100 mm after 185 time steps. (b) *E*-field diagram seen above a sheet 150 by 100 mm after 485 time steps.
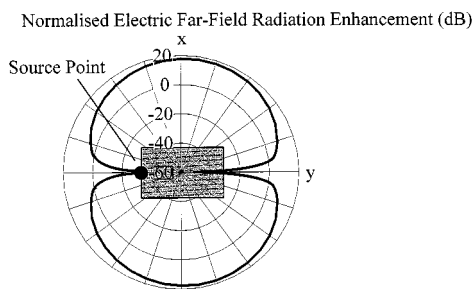

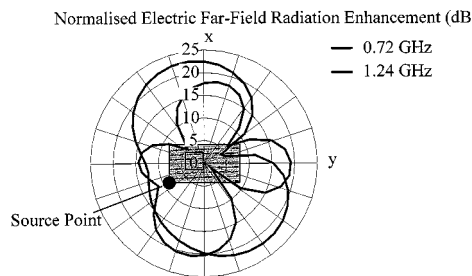Fig. 7. Radiation pattern at 0.72 GHz for a 150-by-100 mm sheet.

Fig. 8. Radiation patterns of the corner excited sheet.

heatsink. We know from the one-dimensional (1-D) case that such a source, perpendicular to the plate, produces maximum excitation when placed at one end of the plate. In a flat sheet, the dominant resonant mode is that corresponding to the half wavelength of the longest dimension which we will refer to as "length". As the width is increased with respect to the length, this dominant mode is affected, and the possibility arises of resonating modes across the width. Fig. 5 shows the effect of

varying the width of the plate relative to the length. The source was placed normal to the sheet in the center at one end. Such a source provides maximum excitation of the length and minimum excitation of the width. Increasing the width of the plate caused the amplitude and frequency of the radiation enhancement to decrease. In the case of the 200-mm sheet with excitation at one end, the RF enhancement was 31 dB at a length:width ratio of 20:1, and this dropped to 21 dB at a ratio of 2:1. This
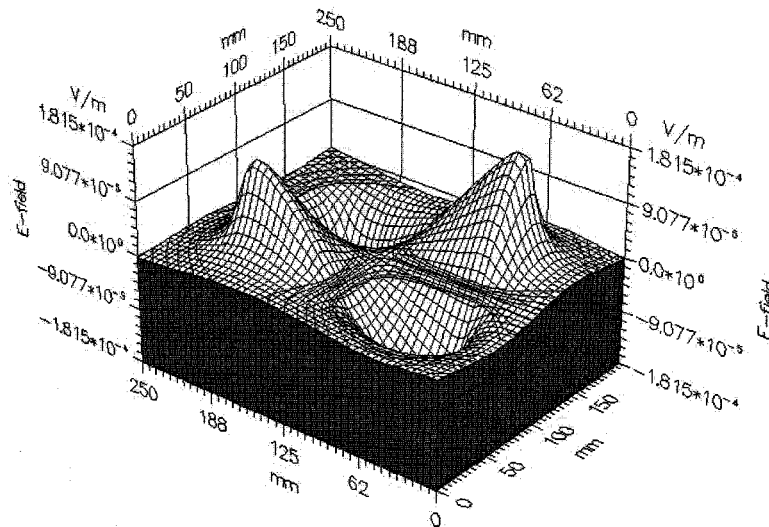
Fig. 9. E-field diagram seen above a corner excited sheet 150 by 100 mm after 620 time steps.

is due to two effects which can be explained by examination of the near field; see Fig. 6. Initially, the majority of the radiation propagates along the edge of the sheet, which can be seen in Fig. 6(a); this increases the path length for the radiaiton, lowering the resonant frequency. After some time, however, the radiation begins to propagate more on the surface of the sheet Fig. 6(b), this results in a higher resonant frequency, closer to the 1-D case of a wire of equivalent length. This spread in frequency over time tends to lower the amplitude of resonance at the dominant mode, this effect was found to be more significant for higher modes. If the width of the sheet is significant compared to the length, then it is likely that a second mode of excitation is possible across the width of the sheet. The far-field radiation pattern gives a clear indication as to which mode is being excited and the direction of excitation. To demonstrate this, a sheet 150 by 100 mm, was chosen. Initially, the source was placed in the center of one end of the longest dimension to excite the longer dimension and not the shorter. For the far-field radiation pattern, Fig. 7 shows the directional nature of the radiation at the resonant frequency. Even though the ratio of width to length is close to 1:1, the sheet behaves like a dipole with the same orientation as the longest dimension of the sheet. As the length-to-width ratio is changed, the radiation pattern changes in frequency and magnitude, but the shape remains the same. This is due to the source position, exciting longitudinal and not transverse modes. When the source was moved from the center of one end, to the corner of the sheet this excited resonances in both directions producing the far-field radiation pattern shown in Fig. 8. At the dominant resonance of the sheet (0.72 GHz), the effect of moving the source has introduced a slight distortion in the radiation pattern, but it still approximates to that produced by a dipole. When a higher frequency is examined at 1.24 GHz, we can see that both of the dimensions have been excited, thus producing a response with four nulls. Again, a slight distortion due to the position of the source is visible. Examination of the near E field above the sheet with the source moved to the corner clearly shows the resonance in both directions of the sheet; see Fig. 9. Thickening the sheet to form a block has a similar effect to that of widening the sheet, the resonances are reduced again in
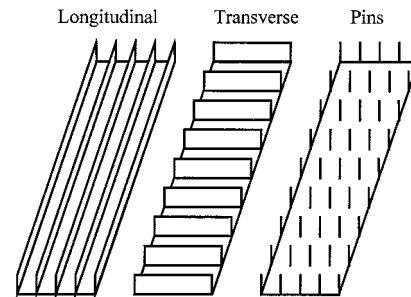

Fig. 10.   Fin orientation for test structures.

both frequency and amplitude, and the bandwidth is increased. Modes in the third dimension may also be excited.

VI. EFFECTS OF FINS

Most heatsinks have some arrangement of fins to increase the surface area as this greatly improves the thermal efficiency. Adding fins to the structure lengthens the path by which the current travels and has the effect of reducing any resonant frequencies. As expected, the length of the fins affects the resonant points. However, the orientation of the fins also has an effect. A thin sheet 200-mm long, 20-mm wide was chosen so that the fundamental mode along the length of the strip would dominate the radiation enhancement with little interference from orthogonal modes. The source was mounted centrally at one end, normal to the plane of the strip. The radiation enhancement was calculated for the strip with and without fins. Three types of fins were used, which are illustrated in Fig. 10, i.e., longitudinal fins running the length of the strip, transverse fins running across the width of the strip, and pins. In all cases, the addition of fins lowered the resonant frequency but not always the amplitude, as shown in Fig. 11. If the fins are mounted longitudinally, then, the effect on the dominant resonance along the length is to reduce the magnitude of the enhancement; e.g., for 20-mm high fins, the radiation enhancement was reduced by approximately 3 dB. This result is similar to that which would be obtained if the plate were changed to a solid block 20-mm high. If, however, the fins

Normalised Electric Far-Field Radiation
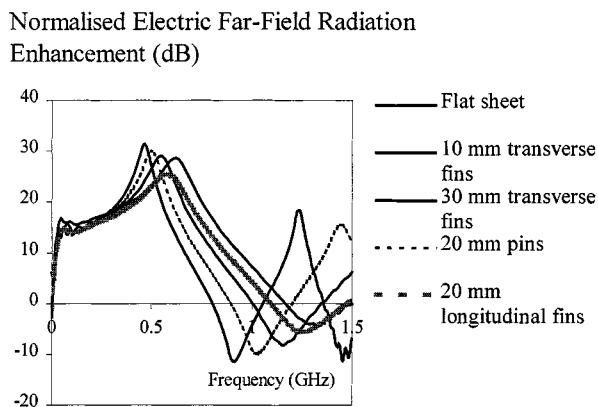Enhancement (dB)

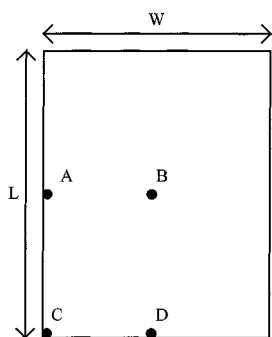Fig. 11.   The effect of adding fins to a flat sheet, 20 by 200 mm.

Fig. 12.   Plan view indicating source positions.

are transversely mounted, then, the magnitude of the resonance is increased; e.g., for 20 mm fins, the radiation enhancement increases by 1.5 dB. When longer fins were used, the effects seen were larger, both increasing the radiation enhancement for transverse fins, and suppressing the enhancement for longitudinal fins. In the case where pins were used instead of fins, the result was similar to that for transverse fins, the magnitude of the resonance was increased whilst reducing the frequency.

VII. A STUDY OF SOME STANDARD HEATSINKS

A number of power heatsinks, selected from those listed in a recent catalogue, were modeled. The structure of each heatsink was coded into the mesh and the source applied at different positions, as indicated in Fig. 12. Many power heatsinks have specific slots for mounting devices whilst others have a flat base which can be drilled to accept devices. In all of the tests, the source positions were representative of realistic positions for mounting devices. The heatsinks were fabricated from extruded aluminum and in all cases the length (L) denotes the extruded dimension. The results are listed in Table I, along with the dimensions of the various heatsinks. The first heatsink examined had a square base of side length 300 mm. The results mirror the findings of the study in Section V since source positions A and D yielded similar results, but with a lower amplitude when the source was at D, due to fin orientation, as shown in Fig. 13. As expected, a source placed in position B, does not excite any significant resonances. It is interesting, however that when the source is moved to position C, the amplitude at 320 MHz is 10 dB higher than the average of the cases for A and D. The longitudinal and transverse modes act together
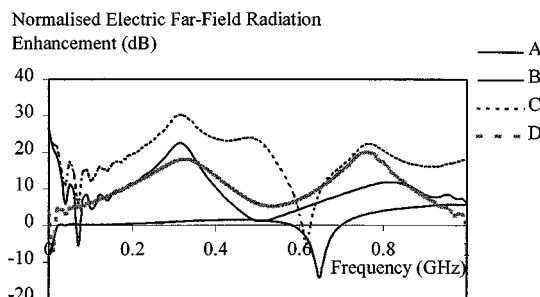
Normalised Electric Far-Field Radiation
Enhancement (dB)

Fig. 13.   Resonant response from test no. 1.

Normalised Electric Far-Field Radiation
Enhancement (dB)

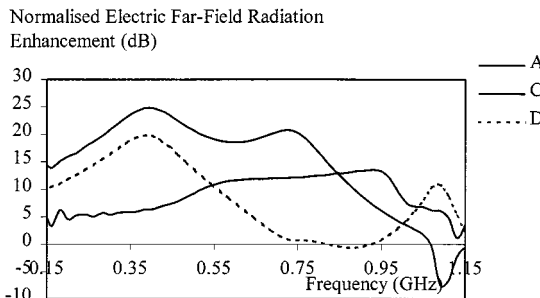Fig. 14.   Resonant response from test no. 2.

Normalised Electric Far-Field Radiation
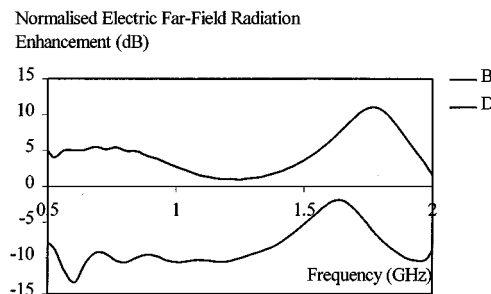Enhancement (dB)

Fig. 15.   Resonant response from test no. 3.

constructively to provide greater enhancement. A similar situation occurred in test 2, where sources positioned at A & D excited resonances due to the width and length, respectively but a source positioned at C produced the greatest response as illustrated by Fig. 14. This heatsink has a much larger length-to-width ratio than that in test 1, and the result is that the longitudinal resonance is of greater magnitude. The resonance across the width is much less in magnitude, however, the Q being very low and making the resonant frequency hard to define. In test 3, the heatsink was finned on both sides and had a central channel on which components could be mounted. Only positions B and D were tested as being realistic source points and the results are shown in Fig. 15. The central channel means that component placement is limited to situations where the fins are longitudinal, and so suppress the radiation. Even when the source was mounted on the edge of the heatsinks, the radiation enhancement was still only 11 dB, nearly 20 dB lower than the other heatsinks modeled. This style of heatsink has obvious advantages but the component placement is limited and the central channel itself can also be a source of resonance.

Previously published measurements taken from a heatsink with a source mounted at position B on the finned side of the

TABLE I
RESULTS FROM THE HEATSINK STUDY

Test No.	Extrusion profile	Source Position, (see Figure 12 for definitions)	Dimensions L, W, H (mm)	Gain at resonant frequencies
1		Position A, on the unfinned side	300, 300, 40	22.5dB @ 310MHz
		Position D, on the unfinned side		18.1dB @ 330MHz, 20.1dB @ 760 MHz
		Position C on the unfinned side		30.2 dB @ 320MHz
2		Position A, on the unfinned side	250, 115, 63	13.5dB @ 930MHz
		Position C, on the unfinned side		24.8dB @ 400MHz
		Position D on the unfinned side		19.8dB @ 380 MHz
3		Position B, in the central channel	87.5, 108, 58.7	-2.1dB @ 1.8GHz
		Position D, in the central channel		11.0dB @ 1.7 GHz
4		Position A, on the unfinned side	100, 120, 37	14.0 dB @ 600MHz
		Position B, on the finned side		7.5 dB @ 4.2 GHz
5		Position C, on the unfinned side	100, 65, 20	18.3dB @ 864MHz
		Position A, on the unfinned side		8.2dB @ 985MHz
		Position B, on the finned side		8.7dB @ 3.89GHz

heatsink, indicated a gain of up to 7.5 dB at 4.2 GHz [3]. These results are shown here as test 4 in Table I. The resonant frequency of the channel is determined by its width, and the Q of the resonance is determined by the ratio of the side area of the channel to its width. Test 5 features a similar heatsink, finned on one side with a central channel. Again, the greatest excitation occurred with the source at position C, and placing the source on the finned side in position B suppressed the resonances, until the channel itself became resonant at 3.89 GHz.

VIII. USING HEATSINKS IN PRACTICE

It has already been demonstrated that the heatsinks employed in power electronics have the capacity to enhance the radiation produced by semiconductor devices mounted on them [3], [4], and the effects of shape, geometry, and component placement on the RF radiation enhancement have been examined using FDTD. It is clear that to reduce the emissions from heatsink-mounted devices, the resonant frequencies of the heatsink should not be excited by the electronic systems incorporating the heatsink. In this paper, it has been shown that it is possible to minimize this enhancement by paying close attention to the shape of the heatsink used and the position of the source on the heatsink. The most common form of heatsink examined here comprises a flat base, on which the components are mounted, with fins on the opposite side to aid heat dissipation. The base is often used as part of the case, or, as a chassis to provide structural integrity as well as thermal conduction. The heatsink has groups of resonant modes where frequencies are related to the length and width of the base. If the ratio of length to width is particularly high, greater than 1:4 say, then, it is likely that only modes along the length will be excited. If this ratio increases, then, the magnitude and Q of the excitation will also increase as the heatsink approaches a dipole in structure. It is clear then that heatsinks with length and width of the same order of magnitude are preferable, the exception being the case when the heatsink is square, as then the modes along both length and width can act together to increase the amplitude of the resonance. Excitation of the structure can occur due to capacitive coupling of energy from devices mounted onto the

heatsink. Hence, the devices should not be mounted close to the edge of the heatsink but nearer the center of the base. This is contrary to common practice, as often, devices are mounted on the edge of the base for ease of manufacture. If the devices are closer to the center, then, the thermal performance will be better and the emissions produced will be less likely to excite the resonances of the heatsink. The addition of fins to heatsinks is common, as this increases the surface area, thus reducing the thermal resistance. Fins also affect the resonant behavior of the heatsink, since their presence lowers the frequency of the dominant resonance, and affects the amplitude, depending upon the orientation of the fins. If the fins run in the direction of the dominant dimension, then, they reduce the resonant effects of the heatsink; if however they run perpendicular to the dominant dimension, then, they will increase the resonant effects such that the longer the fins the greater the effect. If the heatsink has pins rather than fins, then, the effect is to increase the resonance by a similar amount to the case where the fins are perpendicular to the dominant direction. Some heatsinks have large channels in which components are mounted. This type of heatsink is especially common with the TO3 type of semiconductor casing, where the component is mounted on the finned side of the heatsink, usually external to the case of the equipment. This channel can act as a resonant cavity although this is likely to be at a frequency which is higher by an order of magnitude than the resonant frequencies of the base. In previous work [3], the authors have shown, by modeling and measurements carried out on a heatsink, that the width of the channel determines the frequency of the radiation enhancement whilst the length and height of the channel determine the magnitude and directional selectivity of the radiation. Tests have also shown that if the channel is broken up by one or more slots there is very little change in the frequency response. This paper only examines the response of the heatsink to single sources. In the majority of circuits employing power heatsinks, there will be a number of sources acting on the heatsink. These sources will have combined resonant effects which increase the electromagnetic fields propagating around the heatsink. Another problem yet to be examined is that of coupling from one device to another. Component placement may be such that the EM radiation from

one device couples to the gate of another device thus causing spurious switching and associated failures. Of most concern are the large heatsinks, used extensively in power conversion applications, since it is these which are liable to have a large number of components, prone to EM radiation mounted onto them. The resonant frequencies of these heatsinks are liable to be excited by the EMI produced by the electronics, if the frequencies of excitation and the resonant frequencies are both within the range covered by current EMC regulations then careful choice of the heatsink and orientation of components will have a significant effect on the radiated emissions.

REFERENCES

[1] K. Li, C. F. Lee, S. Y. Poh, R. T. Shin, and J. A. Kong, "Application of FDTD method for analysis of electromagnetic radiation from VLSI heatsink configurations," *IEEE Trans. Electromagn. Compat.*, vol. 35, pp. 204–214, May 1993.

[2] C. E. Brench, "Heatsink radiation as a function of geometry," in *Proc. IEEE Int. Symp. Electromagnetic Compatibility*, Chicago, IL, 1994, pp. 105–109.

[3] N. J. Ryan, D. A. Stone, and B. Chambers, "Application of the FDTD method to modeling the electromagnetic radiation from heatsinks," in *Proc. IEE 10th Int. Conf. Electromagnetic Compatibility, EMC'97*, Sept. 1–3, 1997, pp. 119–124.

[4] N. J. Ryan, D. A. Stone, and B. Chambers, "Application of FDTD to the prediction of RF radiation from heatsinks," *Electron. Lett.*, vol. 33, no. 17, pp. 1443–1444, 1997.

[5] K. S. Yee, "Numerical solution of initial boundary value problems involving Maxwell's equations in isotropic media," *IEEE Trans. Antennas Propagat.*, vol. AP-14, pp. 302–307, Apr. 1966.

[6] A. Taflove, *Computational Electrodynamics*. Norwell, MA: Artech House, 1995.

[7] G. Mur, "Absorbing boundary conditions for finite-difference approximation of the time-domain electromagnetic field equations," *IEEE Trans. Electromagn. Compat.*, vol. EMC-23, pp. 337–382, Aug. 1981.

[8] R. J. Luebbers, K. S. Kunz, M. Schneider, and F. Hunsberger, "A finite-difference time domain near zone to far zone transformation," *IEEE Trans. Antennas Propagat.*, vol. 39, pp. 429–433, Apr. 1991.

[9] D. M. Hockanson, J. L. Drewniak, T. H. Hubing, and T. P. Van Doren, "FDTD modeling of common-mode radiation from cables," *IEEE Trans. Electromagn. Compat.*, vol. 38, pp. 376–387, Aug. 1996.

[10] R. A. Burberry, *VHF and UHF Antennas*. Stevanage, U.K.: Peregrinus, 1992.

[11] J. D. Kraus, *Electromagnetics*, 4th ed. New York: McGraw Hill, 1992.

Nick J. Ryan (M'98) received the B.Eng. degree from the University of Bristol, Bristol, U.K., in 1990, and the Ph.D. degree from the University of Sheffield, Sheffield, U.K., in 1998, both in electrical and electronic engineering.

He joined the department of engineering in the University of Aberdeen, Aberdeen, U.K., in 1997, where he currently lectures about safety and reliability in electronic systems. His research interests include computational electrodynamics, electromagnetic compatibility, and renewable energy systems.

Barry Chambers (SM'99) received the Ph.D. degree in electrical engineering from the University of Sheffield, Sheffield, U.K., in 1969.

Following a period at the University of British Columbia, Vancouver, BC, Canada, he returned to University of Sheffield, where is now Professor of radio frequency and microwave engineering in the Department of Electronic and Electrical Engineering and Head of the Communications and Radar Research Group. His current research interests include EMC, radio frequency and microwave metrology, electromagnetic wave scattering and novel smart electromagnetic materials and structures for application in low observable technology, EMC shielding, and communication systems.

Dr, Chambers is a Chartered Engineer and a Fellow of the Institute for Electrical Engineers, U.K.

D. A. Stone received the B.Eng. degree in electronic engineering from the University of Sheffield, Sheffield, U.K., in 1984, and the Ph.D. degree from Liverpool University, Liverpool, U.K., in 1989.

In 1989, he joined the University of Sheffield as a member of academic staff, specializing in power electronics and machine drive systems. His current research interests are in hybrid-electric vehicles, battery charging, EMC, and novel lamp ballasts for low pressure fluorescent lamps.